Proc. Natl. Acad. Sci. USA
Vol. 88, pp. 281–285, January 1991
Neurobiology

Recombinant human nerve growth factor is biologically active and labels novel high-affinity binding sites in rat brain

(neurotrophic factor/receptor binding/cholinergic neurons/caudate-putamen)

C. ANTHONY ALTAR*†, LOUIS E. BURTON‡, GREGORY L. BENNETT§, AND MILLICENT DUGICH-DJORDJEVIC*

Departments of *Developmental Biology, ‡Recovery Process Research and Development, and §Immunology Research and Assay Technology, Genentech, Inc., South San Francisco, CA 94080

Communicated by James L. McGaugh, August 27, 1990 (received for review April 30, 1990)

ABSTRACT **Iodinated recombinant human nerve growth factor (^{125}I-rhNGF) stimulated neurite formation in PC12 cell cultures with a half-maximal potency of 35–49 pg/ml, compared with 39–52 pg/ml for rhNGF. In quantitative ligand autoradiography, the *in vitro* equilibrium binding of ^{125}I-rhNGF to brain sections showed a 10-fold regional variation in density and was saturable, reversible, and specifically displaced by up to 74% with rhNGF or murine NGF (muNGF). At equilibrium, ^{125}I-rhNGF bound to these sites with high affinity (K_d 52–85 pM) and low capacity (B_{max} ≤13.2 fmol/mg of protein). Calculation of ^{125}I-rhNGF binding affinity by kinetic methods gave average K_d values of 24 and 31 pM. Computer-generated maps revealed binding in brain regions not identified previously with ^{125}I-muNGF, including hippocampus; dentate gyrus; amygdala; paraventricular thalamus; frontal, parietal, occipital, and cingulate cortices; nucleus accumbens; olfactory tubercle; subiculum; pineal gland; and medial geniculate nucleus. NGF binding sites were distributed in a 2-fold increasing medial–lateral gradient in the caudate-putamen and a 2-fold lateral–medial gradient in the nucleus accumbens. ^{125}I-rhNGF binding sites were also found in most areas labeled by ^{125}I-muNGF, including the interpeduncular nucleus, cerebellum, forebrain cholinergic nuclei, caudoventral caudate-putamen, and trigeminal nerve nucleus. ^{125}I-rhNGF binding sites were absent from areas replete with low-affinity NGF binding sites, including circumventricular organs, myelinated fiber bundles, and choroid plexus. The present analysis provides an anatomical differentiation of high-affinity ^{125}I-rhNGF binding sites and greatly expands the number of brain structures that may respond to endogenous NGF or exogenously administered rhNGF.**

The neurotrophic activities of nerve growth factor (NGF) depend upon its binding to the high-affinity (K_d of 10^{-11} M), membrane-bound receptor located on dependent neurons (1, 2) and not to the lower-affinity (K_d of 10^{-9} M), non-neuronal site (3, 4). Thus, a map of high-affinity NGF binding sites in brain will identify the most likely neuronal targets for the neurotrophic actions of NGF. The distribution of NGF receptors (NGFRs) in brain has been studied with emulsion autoradiography using an iodinated murine NGFR (muNGFR) antibody (5–14) or ^{125}I-muNGF (15–19) as ligands. The muNGFR monoclonal antibody 192-IgG recognizes a low-affinity receptor (20) but identification of the high-affinity NGFR with this probe is equivocal (2, 20, 21). Both of these techniques consistently identified NGFRs only in the cholinergic nuclei of the basal forebrain, including the medial septum, diagonal band, and substantia innominata/nucleus basalis. Inconsistent localizations of NGFRs with ^{125}I-muNGF, and discrepancies in receptor localization between the antibody and ligand binding techniques, indicated that technical improvements were necessary before a definitive map of the high-affinity receptors could be made.

Autoradiography of NGFRs with ^{125}I-sensitive x-ray film can quantify the bound ligand (22, 23) and avoid the losses of bound ligand by the ethanol and organic solvent washes used with liquid emulsion autoradiography (24). Our preliminary study with ^{125}I-muNGF and dry film autoradiography revealed specific binding in neocortical and basal ganglia regions not observed with the liquid emulsion technique (15–19). The present studies used dry film autoradiography and biologically active, highly purified ^{125}I-labeled recombinant human NGF (rhNGF) to determine if and where this ligand would bind to slide-mounted adult rat brain sections.

MATERIALS AND METHODS

Production, Purification, and Iodination of rhNGF. Purified (>98%) rhNGF was produced by the Research Collaborations group at Genentech, using transfected Chinese hamster ovary cell cultures and anion-exchange chromatography (25) as described (26, 27). rhNGF stimulated PC12 (rat pheochromocytoma cell line) neurite outgrowth (51) with an EC_{50} value of 39 and 52 pg/ml in two experiments conducted by different personnel in separate laboratories (Fig. 1). rhNGF was iodinated (28) with modifications (26, 27) and used within 1–6 days in all but one study, since decreases in the proportion of total ^{125}I-rhNGF binding that was displaced by 100 nM rhNGF were noted after this time. Two- and 3-week-old ^{125}I-rhNGF (71.6 μCi/μg; 3580 Ci/mmol of rhNGF dimer; 1 Ci = 37 GBq) stimulated neurite outgrowth in the PC12 bioassay with an EC_{50} of 49 ± 19 pg/ml (2-week-old tracer; n = 4) and 49 ± 0.8 pg/ml (3-week-old tracer; n = 3). The 1-day-old batch of tracer produced a half-maximal stimulation of PC12 neurite outgrowth at 35 pg/ml. Without a biochemical separation of labeled and unlabeled species, we cannot exclude the possibility that biological activity is due to unlabeled rhNGF. However, the high degree of rhNGF labeling (1.65:1 ratio of ^{125}I to rhNGF dimer), the retrograde transport of ^{125}I-rhNGF, which can be blocked by rhNGF (26), and the indistinguishable potencies of rhNGF and ^{125}I-rhNGF in the PC12 assay (Fig. 1) indicate that ^{125}I-rhNGF is active in bioassays of NGF function.

Brain Sections. Brains from male Sprague–Dawley rats were frozen in isopentane at −15°C either separately, for anatomical mapping, or as a group of four to five brain hemispheres (22), for association, dissociation, and equilibrium saturation analyses. Sections (12 μm) were thaw-mounted onto gelatin-coated glass microscope slides and stored frozen for up to 1 month at −70°C.

The publication costs of this article were defrayed in part by page charge payment. This article must therefore be hereby marked "*advertisement*" in accordance with 18 U.S.C. §1734 solely to indicate this fact.

Abbreviations: ACh, acetylcholine; ChAT, choline acetyltransferase; CP, caudate-putamen; NGF, nerve growth factor; muNGF, murine NGF; rhNGF, recombinant human NGF; NGFR, NGF receptor.

†To whom reprint requests should be addressed.

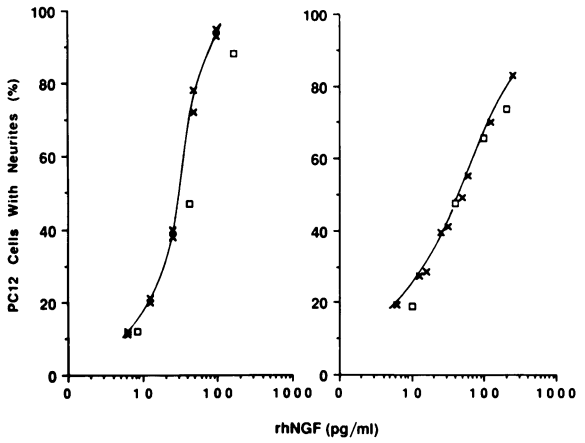

FIG. 1. Stimulation of PC12 cell neurite outgrowth by rhNGF (X) and ^{125}I-rhNGF (□). Values are single (rhNGF) or averages of three to four replicate (^{125}I-rhNGF) EC_{50} determinations. Two independent experiments are shown (*Left* and *Right*).

^{125}I-rhNGF Binding Assay. Binding assays (14) were modified for dry film autoradiography (27). After thawing, each section was preincubated for 3 hr at 22°C in 100 mM phosphate, pH 7.4/200 mM NaCl/0.5 mM $MgCl_2$. Sections were incubated in the same buffer with the addition of cytochrome *c* (1 mg/ml; Sigma), leupeptin (4 μg/ml; Sigma), 0.5 mM phenylmethylsulfonyl fluoride (BRL; first dissolved to 0.1 mg/ml in 2-propanol), and ^{125}I-rhNGF [4–294 pM (equilibrium saturation analysis) or 75–96 pM (all other assays), based on a monomeric molecular weight of 12,500]. Adjacent brain sections were incubated in the same solutions with the addition of 100 nM rhNGF or native muNGF (Biomedical Technologies, Stoughton, MA) to define displaceable binding. After incubation, the sections were washed for 3 min in three changes of buffer at 22°C but were not exposed to formaldehyde vapors or defatted in graded alcohols and xylene (15, 16) or acetone (17) as done for emulsion autoradiography. Equivalent amounts of total and nondisplaceable binding were obtained with 3-min, 10-min, and 2-hr washes with unlabeled buffer (unpublished data). Sections were fixed for 10 min in 4% paraformaldehyde at 22°C, rinsed for 2 sec in water at 22°C, and air-dried.

Image and Data Analysis. The dried sections and ^{125}I autoradiography standards (Amersham) were apposed for 1–6 days to x-ray film (Hyperfilm; Amersham). The developed films were imaged with an RAS 3000 system (Amersham). Ligand concentrations were measured and images of rhNGF-displaced binding were produced with digital subtraction autoradiography (23). Statistical analyses included Dunnett's *t* test following a one-way analysis of variance. Kinetic determinations of K_d values were made assuming pseudo-first-order conditions (29), since <10% of free ligand was bound to sections after the 3-hr incubation. K_d and B_{max} determinations were made according to the best fit to a parabola by iterative, nonlinear regression analysis (30).

RESULTS

The association of displaceable, 4-day-old ^{125}I-rhNGF to the lateral and medial caudate-putamen (CP) (n = 4) increased until 3 hr, at which time equilibrium was achieved and no additional binding was obtained at 4 hr (Fig. 2 *Upper*). The association rate constant (k_1) was 0.0217×10^9 $M^{-1}min^{-1}$ in the lateral CP and 0.188×10^9 $M^{-1}min^{-1}$ in the medial CP. The dissociation of 21-day-old ^{125}I-rhNGF occurred at a rate (k_{-1}) of 4.8×10^{-4} min^{-1} in the lateral CP and 1.08×10^{-3} min^{-1} in the medial CP (Fig. 2 *Lower*). The k_{-1}/k_1 ratio gave equilibrium dissociation constant (K_d) values of 22 and 5.8

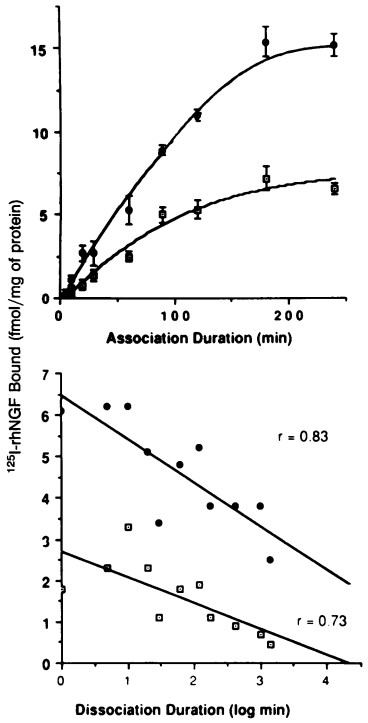

FIG. 2. Time courses of ^{125}I-rhNGF (89 pM) association with (*Upper*) and dissociation from (*Lower*) lateral (●) and medial (□) CP of brain sections. Nondisplaceable binding was defined with 100 nM unlabeled rhNGF. SEM of these determinations was 3–18% (medial CP) and 6–20% (lateral CP). All values are means ± SEM (n = 4–5 brains). r, Correlation coefficient.

pM for the lateral and medial CP, respectively. The binding of 1-day-old ^{125}I-rhNGF to tissue sections (n = 5) varied by 4–20% (SEM) at association time points and by 3–14% at dissociation time points. The k_1 values were 0.0348×10^9 $M^{-1}min^{-1}$ for lateral CP and 0.0195×10^9 $M^{-1}min^{-1}$ for medial CP. The k_{-1} values were 9.0×10^{-4} min^{-1} for lateral CP and 1.11×10^{-3} min^{-1} for medial CP. Determination of K_d by k_{-1}/k_1 gave 26 and 57 pM for the lateral and medial CP, respectively. Average K_d values for the two association/dissociation experiments were 24 and 31 pM for lateral and medial CP, respectively. These values are similar to the K_d estimates obtained with ^{125}I-muNGF (16, 18), and the protracted ligand-dissociation times are consistent with those reported for chick ganglia (31).

The displaceable binding of 4–128 pM ^{125}I-rhNGF to forebrain sections that included the CP and cholinergic nuclei averaged 50% (range 30–74%), as previously reported for ^{125}I-muNGF (15, 17), and decreased to 26% at 294 pM. Nevertheless, the combination of autoradiography with computerized image analysis allowed the calculation of K_d and B_{max} values (Table 1) and displaceable binding (Table 2) with small errors (SEM 3–25% and <10%, respectively). The equilibrium binding of 50–75 pM ^{125}I-rhNGF was inhibited

Table 1. Capacity and affinity of ^{125}I-rhNGF binding to rat forebrain

Brain region	K_d	B_{max}
Lateral CP	52 ± 9	13.2 ± 0.8
Medial CP	70 ± 18	7.2 ± 1.0*
Horizontal diagonal band	85 ± 13	9.4 ± 0.25*

Sections of rat forebrain at the level of the CP were incubated in 5.8–294 pM ^{125}I-rhNGF. The K_d and B_{max} values are means ± SEM of four brains.

*$P < 0.01$ versus lateral CP (Dunnett's *t* test). K_d values did not differ ($P > 0.05$) among the three brain regions.

Table 2. Regional distribution of ^{125}I-rhNGF binding sites from frontal cortex to medulla of rat brain

Brain region	Displaceable ^{125}I-rhNGF	
	fmol/mg of protein	% of total binding
Interpeduncular nucleus	11.0 ± 0.9	74 ± 2
Spinal trigeminal tract (V)	10.8 ± 2.0	61 ± 4
Posterior CP		
Lateral	9.1 ± 0.61*	67 ± 13
Medial	4.1 ± 0.22	48 ± 3
Anterior CP		
Lateral	8.3 ± 0.42*	63 ± 2
Medial	4.6 ± 0.55	52 ± 5
Amygdala	6.9 ± 0.92	67 ± 6
Diagonal band, vertical limb	6.7 ± 0.83	60 ± 5
Nucleus accumbens		
Medial	6.4 ± 0.29*	64 ± 4
Lateral	3.0 ± 0.60	44 ± 8
Olfactory tubercle	5.5 ± 0.55	56 ± 5
CA1 rostral hippocampus	5.6 ± 1.08	57 ± 9
Caudal hippocampus	5.6 ± 1.0	53 ± 9
Medial septum	4.9 ± 1.0	56 ± 10
Dentate gyrus		
Rostral	4.2 ± 1.05	51 ± 11
Caudal	2.7 ± 0.54	42 ± 7
Fundus of CP	4.6 ± 0.26	52 ± 5
Pineal gland	4.4 ± 0.34	33 ± 4
Cingulate cortex	3.9 ± 0.77	46 ± 9
Diagonal band, horizontal limb	3.5 ± 0.43	42 ± 2
Subiculum	3.5 ± 0.55	42 ± 6
Cerebellum, Purkinje layer	3.2 ± 0.24	44 ± 6
Substantia innominata	2.9 ± 0.44	45 ± 5
Occipital cortex	2.7 ± 0.16	44 ± 2
Medial geniculate nucleus	2.5 ± 0.45	41 ± 5
Frontal cortex	2.1 ± 0.22	30 ± 4
Frontoparietal cortex	1.9 ± 0.50	29 ± 7

Coronal sections of four rat brains were collected every 350 μm and incubated in 75 pM ^{125}I-rhNGF alone or with 100 nM rhNGF to define nondisplaceable binding in adjacent sections. Quantitation was done on all brain regions in which binding was reliably displaced by 100 nM rhNGF. Average SEM for all regions was 12.5%.
*$P < 0.01$ compared to adjacent anatomical area (Dunnett's t test).

30–74% by 100 nM rhNGF (Table 2) or muNGF (unpublished data), but not by up to 100 μM cytochrome c, a protein similar in isoelectric point and molecular weight to rhNGF, or 100 nM basic fibroblast growth factor, activin A, recombinant human growth hormone, or insulin-like growth factor I. The SEM associated with the determination of displaceable binding in the 27 areas represented in Table 2 ranged from 2% to 24% and averaged 12.5% ($n = 4$ per brain region).

Digital subtraction autoradiography was used to produce images of displaceable (specific) binding from the images of total and nonspecific binding (Fig. 3). The highest density of sites was found in the interpeduncular nucleus (Table 2), with predominant binding in the midline rostral and lateral nuclei (Fig. 4). Displaceable binding was also high in many other regions, including the spinal trigeminal tract (Table 2) and nucleus (Fig. 4). A 2-fold greater density of ^{125}I-rhNGF binding sites was found in the lateral third compared with the medial third of the CP ($P < 0.01$), at both the anterior and posterior neostriatal levels (Table 2). The densest ^{125}I-rhNGF binding in the anterior CP was in the dorsolateral region and ventrolaterally in the posterior CP (Figs. 3 and 4). In the nucleus accumbens, more ^{125}I-rhNGF binding was present in the medial than in the lateral portion ($P < 0.01$; Table 2). No displaceable binding was detected throughout the corpus callosum, anterior commissure, globus pallidus, thalamus, hypothalamus, substantia nigra, choroid plexus, entorhinal

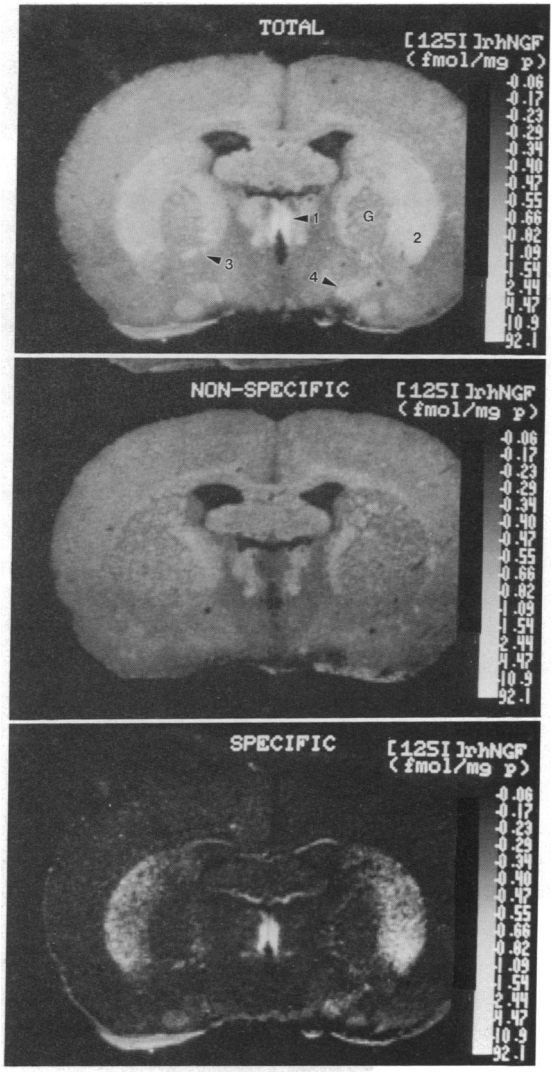

FIG. 3. Image of total, nonspecific, and specific ^{125}I-rhNGF (75 pM) binding at the level of the globus pallidus [G], caudal CP, and horizontal limb of the diagonal band [4]. Gray scale relates image brightness to amount of bound ^{125}I-rhNGF (fmol/mg of protein). Prominent areas of binding in the total binding image include the paraventricular thalamic nucleus [1], ventrolateral CP [2], and substantia innominata [3].

cortex, periaqueductal gray, or olfactory bulb, or in other regions of the pons (including pontine cholinergic nuclei), red nucleus, area postrema, other amygdaloid nuclei, or other myelinated fiber tracts.

DISCUSSION

Characteristics of ^{125}I-rhNGF Binding to Its High-Affinity Site. The 24–85 pM affinity constants measured by both equilibrium saturation and kinetic methods are within the range of values reported for the binding of ^{125}I-muNGF to its high-affinity receptor (3, 16, 18, 31, 32). The 75 pM concentration of labeled rhNGF is 270-fold below the affinity constant reported for the lower-affinity site in basal forebrain homogenates (2, 31–33) and thus would be expected to label few if any of these sites. Indeed, 400–600 pM concentrations of ^{125}I-rhNGF did not increase displaceable binding. The 3- to 10-min washes after exposure to labeled NGF also diminished the likelihood of low-affinity binding (31), and 20-min or 2-hr washes also failed to significantly alter the amount of specifically bound rhNGF in the brain (unpublished data).

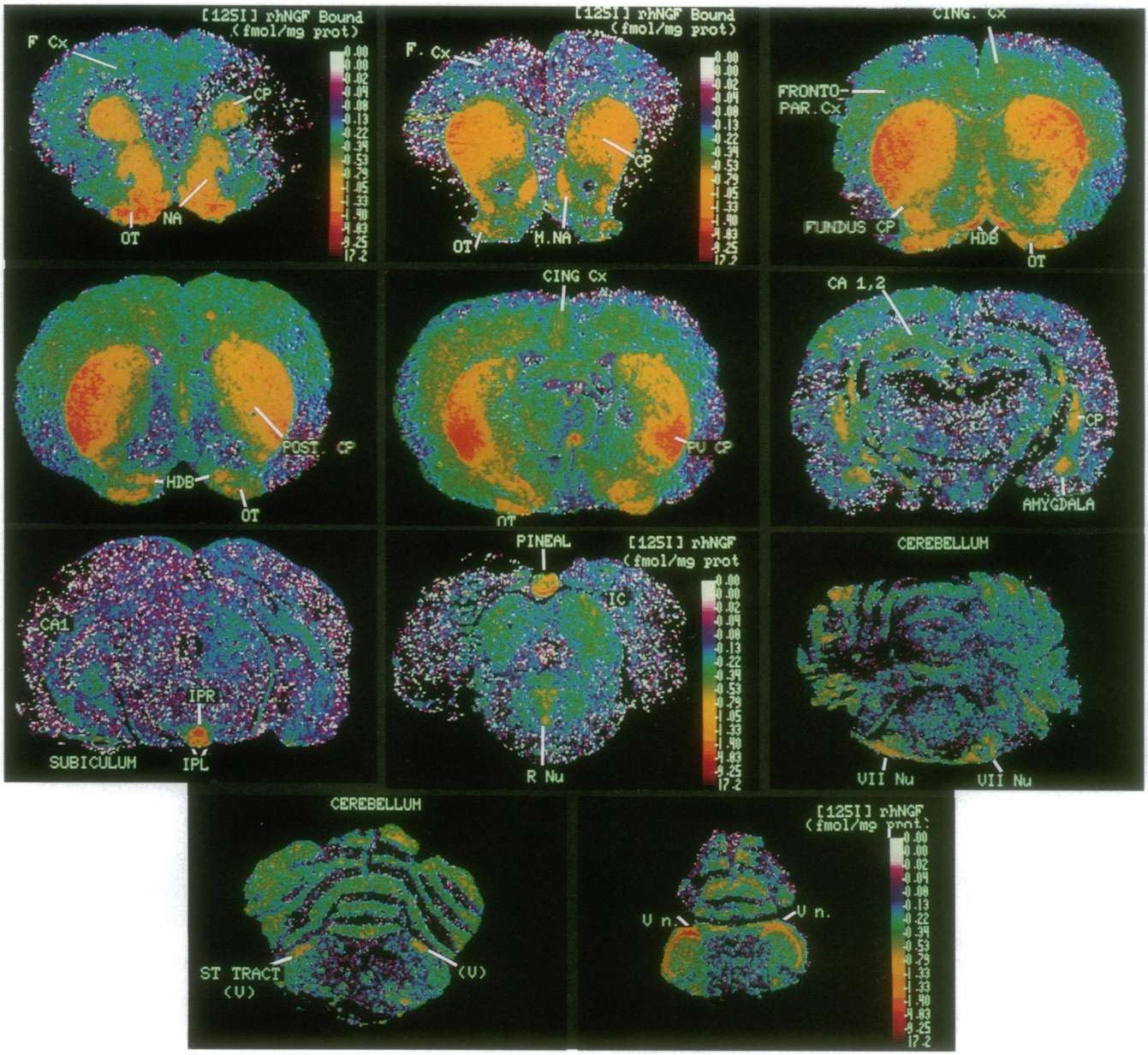

FIG. 4. Quantitative maps of displaceable ^{125}I-rhNGF binding in rat brain achieved by subtracting an image of ^{125}I-rhNGF binding in the presence of 100 nM rhNGF (nondisplaceable binding) from a superimposed image of ^{125}I-rhNGF binding (total binding at 75 pM). Color scale: fmol of displaceable rhNGF bound per mg of protein. CING.Cx, cingulate cortex; CA 1,2, CA1 and -2 of hippocampus; F Cx, frontal cortex; FUNDUS CP, fundus of the CP; FRONTOPAR. Cx, frontoparietal cortex; HDB, horizontal limb of the diagonal band; IC, inferior colliculus; IPL, lateral interpeduncular nucleus; IPR, rostral interpeduncular nucleus; NA, nucleus accumbens; M. NA, medial nucleus accumbens; OT, olfactory tubercle; PV CP, posterior CP; R Nu, raphe nucleus; ST TRACT (V), fifth cranial nerve nucleus and lateral tract; VII Nu, seventh cranial nerve nucleus; V n., fifth cranial nerve nucleus.

Finally, ^{125}I-rhNGF bound to virtually all sites labeled by ^{125}I-muNGF (medial septum, diagonal band, substantia innominata; refs. 16–18) and many additional sites (see below) but did not bind to areas labeled by the monoclonal antibody 192-IgG (circumventricular organs, olfactory bulb, choroid plexus; refs. 34 and 35), most likely because 192-IgG preferentially labels the low-affinity NGFR (2, 20, 21). It is thus likely that the former areas share both high- and low-affinity NGFRs whereas only low-affinity sites are present in the latter regions. Still other regions (neocortex, most of the CP, and nucleus accumbens) were detected here with ^{125}I-rhNGF but were not revealed with NGFR antibodies and are thus relatively enriched with high-affinity NGF binding sites.

The nondisplaceable binding of ^{125}I-rhNGF was 26–70% of the total binding, as observed for ^{125}I-muNGF binding to tissue sections (15, 17), cultured cells (3), and homogenates (16). The maximal capacities of ^{125}I-rhNGF binding measured for the diagonal band and CP were within (33) or exceeded (17) the range of values reported for this high-affinity, low-capacity site in homogenates of the basal forebrain. The lack of B_{max} determinations with prior autoradiographic studies (15–19) prevents a comparison with the values obtained here.

Distribution of NGF Binding Sites. In general, the topography of ^{125}I-rhNGF binding to forebrain sections was similar to the distribution of numerous cholinergic markers, including [^{3}H]vesamicol, a marker for the vesicular acetylcholine (ACh) transporter in central cholinergic nerves (36, 37); the ACh synthetic enzyme, choline acetyltransferase (ChAT) (38, 39); the ACh degradative enzyme, acetylcholinesterase (38); and ACh itself (50). NGF binding was dense in the cholinergic cell body regions (medial septum, diagonal band, substantia innominata) as identified previously with both

NGFR antibodies (7, 11–14, 34, 40) and ^{125}I-muNGF (16–18) and localized to cholinergic cell bodies and dendrites. As in those studies, ^{125}I-rhNGF labeling was also found in the fifth cranial nerve nucleus, spinal trigeminal tract, and caudoventral CP. The laminar arrangement of ^{125}I-rhNGF binding in the cerebellum, also found with ^{125}I-muNGF, is consistent with the discrete localization of NGFRs to the Purkinje cell layer (9, 19). NGF binding was found in the globus pallidus by either technique but not in the present study. The reason for this discrepancy is unclear.

A number of hindbrain areas known to contain cholinergic markers were devoid of ^{125}I-rhNGF binding as was demonstrated with NGFR antibody (8, 34, 40) and direct muNGF binding techniques (15, 18). These "NGFR-poor" cholinergic areas include cranial nerve nuclei III and IV; the pedunculopontine or parabrachial cholinergic projections to thalamus, hypothalamus, and inferior colliculus; the projection of preoptic magnocellular cholinergic neurons to the ventral tegmental area; the innervation of substantia nigra from the anterior commissure; projections from red nucleus and lateral vestibular nucleus to the cerebellum; and projections from the diagonal band to piriform cortex, habenula, and entorhinal cortex (41–44).

High-affinity binding sites for ^{125}I-rhNGF were also identified in the medial and lateral nucleus accumbens, the olfactory tubercle, dorsal hippocampus, the CA1 field of hippocampus, the subiculum, dentate gyrus, cingulate cortex, frontal, parietal, and occipital cortices, amygdala, fundus of the CP, medial geniculate nucleus, paraventricular thalamic nucleus, and the pineal gland. Binding of ^{125}I-muNGF to an "interpeduncular region" was mentioned in one report (16) and identified here as the rostral and lateral interpeduncular nuclei. Interestingly, the interpeduncular nucleus has not only the highest density of ^{125}I-rhNGF binding in rat brain but also the densest cholinergic innervation (43). The 2-fold medial–lateral gradient of increasing NGFR density in both rostral and caudal CP parallels neostriatal gradients of ChAT (45), high-affinity [^{3}H]choline uptake (46), and the density of the ACh-transporter ligand [^{3}H]vesamicol (36). That each of these markers and ^{125}I-rhNGF binding are highest in the dorsolateral part of the rostral CP and ventrolateral portion of the caudal CP is consistent with the colocalization of ChAT with a sparse population of ^{125}I-muNGF binding sites in the ventral neostriatum (18, 34, 40). In the nucleus accumbens, the lateral–medial gradient of increasing cholinergic innervation (37) is opposite to that seen in the neostriatum, and this matches the increasing lateral–medial gradient observed here for NGF binding. The location of NGFRs throughout the neostriatum is consistent with the ability of intraventricularly administered muNGF antibodies to label medial neostriatal cholinergic interneurons (47) and the ability of intraventricularly (48) or locally (49) applied rhNGF to augment ChAT activity in the adult rat neostriatum. These findings predict that exogenously administered NGF may affect cholinergic neurons in the lateral CP and medial nucleus accumbens to a greater extent or at lower doses than in other neostriatal areas. In addition to the neostriatum, the many other brain areas shown here to contain high-affinity rhNGF binding sites greatly expand the number of brain areas in which NGF may function as an endogenous neurotrophic factor or that may respond to exogenous delivery of this potential therapeutic agent.

We greatly appreciate the expert execution of the PC12 assay by Lisa Tealer and James Lofgren.

1. Thoenen, H. & Barde, Y.-A. (1980) *Physiol. Rev.* **60,** 1284–1335.
2. Springer, J. E. (1988) *Exp. Neurol.* **102,** 354–365.
3. Bernd, P., Martinez, H. J., Dreyfus, C. F. & Black, I. B. (1988) *Neuroscience* **26,** 121–129.
4. DiStefano, P. S. & Johnson, E. M. (1988) *J. Neurosci.* **8,** 231–241.
5. Gomez-Pinilla, G., Cotman, C. W. & Nieto-Sampedro, M. (1989) *Brain Res.* **479,** 252–262.
6. Hefti, F., Hartikka, J., Salvatierra, A., Weiner, W. J. & Mash, D. C. (1986) *Neurosci. Lett.* **69,** 37–41.
7. Kiss, J., McGovern, J. & Patel, A. J. (1988) *Neuroscience* **27,** 731–748.
8. Kordower, J. H., Bartus, R. T., Bothwell, M., Schatteman, G. & Gash, D. M. (1988) *J. Comp. Neurol.* **277,** 465–486.
9. Pioro, E. P. & Cuello, A. C. (1988) *Brain Res.* **455,** 182–186.
10. Schatteman, G. C., Gibbs, L., Lanahan, A. A., Claude, P. & Bothwell, M. (1988) *J. Neurosci.* **8,** 860–873.
11. Taniuchi, M., Schweitzer, J. B. & Johnson, E. M., Jr. (1986) *Proc. Natl. Acad. Sci. USA* **83,** 1950–1954.
12. Dawborn, D., Allen, S. J. & Semenenko, F. M. (1988) *Neurosci. Lett.* **94,** 138–144.
13. Hefti, F. (1986) *J. Neurosci.* **6,** 2155–2162.
14. Hefti, F. & Mash, D. C. (1989) *Neurobiol. Aging* **10,** 75–87.
15. Raivich, G. & Kreutzberg, G. W. (1987) *Neuroscience* **20,** 23–36.
16. Richardson, P. M., Issa, V. M. & Riopelle, R. J. (1986) *J. Neurosci.* **6,** 2312–2321.
17. Richardson, P. M., Verge, V. M. K. & Riopelle, R. J. (1989) in *Nerve Growth Factors*, Int. Brain Res. Org. Handbook Series: Methods in the Neurosciences, ed. Rush, R. A. (Wiley, New York), Vol. 12, pp. 315–327.
18. Riopelle, R. J., Richardson, P. M. & Verge, V. M. K. (1987) *Neurochem. Res.* **12,** 923–928.
19. Cohen-Cory, S., Dreyfus, C. F. & Black, I. B. (1989) *Exp. Neurol.* **105,** 104–109.
20. Chandler, C. E., Parsons, L. M., Hosang, M. & Shooter, E. M. (1984) *J. Biol. Chem.* **259,** 6882–6889.
21. Green, S. H. & Green, L. A. (1988) *J. Biol. Chem.* **261,** 15316–15326.
22. Altar, C. A. (1988) in *Receptor Localization: Ligand Autoradiography*, eds. Leslie, F. & Altar, C. A. (Liss, New York), pp. 191–208.
23. Altar, C. A., Walter, R. J., Neve, K. A. & Marshall, J. F. (1984) *J. Neurosci. Methods* **10,** 173–188.
24. Kuhar, M. J. & Unnerstall, J. R. (1982) *Brain Res.* **244,** 178–181.
25. Darling, T. J. & Shooter, E. (1984) *Methods for Serum-Free Culture of Neuronal and Lymphoid Cells* (Liss, New York), pp. 79–93.
26. Altar, C. A. & Bakhit, C., *Brain Res.*, in press.
27. Altar, C. A., Dugich-Djordjevic, M., Armanini, M. & Bakhit, C., *J. Neurosci.*, in press.
28. De Larco, J. E., Preston, Y. A. & Todaro, G. J. (1980) *J. Cell. Physiol.* **109,** 143–152.
29. Weiland, G. A. & Molinoff, P. B. (1981) *Life Sci.* **29,** 313–330.
30. Bliss, C. I. & James, A. T. (1966) *Biometrics* **22,** 573–580.
31. Sutter, A., Riopelle, R. J., Harris-Warrick, R. M. & Shooter, E. M. (1979) *J. Biol. Chem.* **254,** 5972–5982.
32. Korsching, S., Auburger, G., Heumann, R., Scott, J. & Thoenen, H. (1985) *EMBO J.* **4,** 13890–13903.
33. Alberch, J., Carman-Krzan, M. & Wise, B. C. (1989) *Soc. Neurosci. Abstr.* **15,** 869.
34. Woolf, N. J., Gould, E. & Butcher, L. (1989) *Neuroscience* **30,** 143–152.
35. Yan, Q., Wanaka, A., Clark, H. B. & Johnson, E. M. (1989) *Soc. Neurosci. Abstr.* **15,** 864.
36. Marien, M. R., Parsons, S. M. & Altar, C. A. (1987) *Proc. Natl. Acad. Sci. USA* **84,** 876–880.
37. Altar, C. A. & Marien, M. R. (1988) *Synapse* **2,** 486–493.
38. Hoover, D. B., Muth, E. A. & Jacobowitz, D. M. (1978) *Brain Res.* **153,** 295–306.
39. Kobayashi, R. M., Brownstein, M., Saavdra, J. M. & Palkovits, M. J. (1975) *J. Neurochem.* **24,** 633–640.
40. Kiss, J. & Patel, A. J. (1989) *Neurosci. Lett.* **105,** 251–256.
41. Paxinos, G. & Butcher, L. L. (1985) in *The Rat Nervous System*, ed. Paxinos, G. (Academic, New York), Vol. 1, pp. 487–522.
42. Fibiger, H. C. (1982) *Brain Res. Rev.* **4,** 327–388.
43. Kasa, P. (1986) *Prog. Neurobiol.* **26,** 211–272.
44. Satoh, K., Armstrong, D. M. & Fibiger, H. C. (1983) *Brain Res. Bull.* **11,** 693–720.
45. Guyenet, P., Euvrard, C., Javoy, F., Herbert, A. & Glowinski, J. (1977) *Brain Res.* **136,** 487–500.
46. Rea, M. A. & Simon, J. R. (1981) *Brain Res.* **219,** 317–326.
47. Schweitzer, J. B. (1989) *Brain Res.* **490,** 390–396.
48. Hagg, T., Hagg, F., Vahlsing, H. L., Manthorpe, M. & Varon, S. (1989) *Neuroscience* **30,** 95–103.
49. Armanini, M., Feinglass, S., Altar, C. A. & Bakhit, C. (1990) *Soc. Neurosci. Abstr.* **16,** 478.
50. Cheney, D. L., LeFevre, H. F. & Racagni, G. (1975) *Neuropharmacology* **14,** 801–809.
51. Greene, L. A. & Rukenstein, A. (1989) in *Nerve Growth Factors*, ed. Rush, R. A. (Wiley, New York), pp. 139–149.